Journal of Applied Polymer Science

Nanocomposites Based on MWCNT and Polystyrene, Styrene-Acrylonitrile Copolymer, or Polymethylmethacrylate, Obtained by Miniemulsion Polymerization

Dan Donescu,[1] Mihai Cosmin Corobea,[1] Cristian Petcu,[1] Catalin Ilie Spataru,[1] Marius Ghiurea,[1] Raluca Somoghi,[1] Raluca Gabor,[1] Jean-Michel Thomassin,[2] Michaël Alexandre,[2] Christine Jerome[2]

[1]Polymer Department, National Institute for Research & Development in Chemistry and Petrochemistry–ICECHIM Bucharest, 060021, Romania

[2]Department of Chemistry, Center for Education and Research on Macromolecules (CERM), University of Liege (ULg), 4000, Belgium

Correspondence to: M. C. Corobea (E-mail: mcorobea@yahoo.com)

ABSTRACT: Free radical miniemulsion polymerization of styrene (St), St/acrylonitrile 3 : 1 mixture or methylmethacrylate in the presence of multiwalled carbon nanotubes (MWCNT) was proven as a convenient way to obtain homogenous hybrids with perspectives in associated applications like foams specialties materials. Miniemulsion polymerization was viable up to 2% wt. MWCNT to monomer, without agglomerations. The grafting on MWCNT during the polymerization occurs without the need for supplementary functionalization and the polymer grafted nanotubes showed stable dispersions in the polymer solvent. Monomer polarity affected the grafting ability during the polymerization process. The nanocomposites obtained after purification and drying were used in foaming process. MWCNT presence in the related nanocomposites decreased the pore sizes in foam-like materials (for all three different matrices). At 1 wt % MWCNT content, low density (< 0.3 g/cm^3), low pore size (< 10 μm) and high cell density ($>10^9$ cell/cm^3) were achieved. © 2014 Wiley Periodicals, Inc. J. Appl. Polym. Sci. **2014**, *131*, 41148.

KEYWORDS: applications; composites; foams; graphene and fullerenes; nanotubes; radical polymerization

Received 5 March 2014; accepted 6 June 2014
DOI: 10.1002/app.41148

INTRODUCTION

Twenty years following Iijima's report on the synthesis of carbon nanotubes (CNT),[1] these materials are still of considerable interest for use as fillers in polymeric nanocomposites. In the last five years, a considerable number of review articles have been published that have attempted to organize the results obtained in this field.[2–17] Unlike other types of nanofillers (nanoparticles and layered silicates), CNTs exhibit the greatest "aspect ratio" (AR) value, which is the ratio between the longest and shortest axes,[10] and the lowest polarity among the other classes of particles. These two characteristics consequently induce a weak dispersion of the CNTs in more polar polymer matrices and a reduced ability in dispersing up to the elementary particle level.[11] Investigations on the influence of the AR of CNTs have demonstrated that the best performances for the final nanocomposites can be attained by maximizing only this parameter. Another issue associated with the processing of CNTs in polymer matrices is that increasing the AR results in a weaker CNT dispersion capacity.[14–17]

The polarity differences between nanofillers and monomers can be assisted by surface modifications and phase partition as well, to increase the dispersion between phases.[18–20] Covalent and noncovalent functionalization of nanofillers has been explored to remove the barriers imposed by the polarity difference between the CNTs and polymeric matrices.[4,8,13] Several dispersion methods have been investigated for modifying surfaces in specific manners without affecting the AR value of the CNTs.[4]

Seeking an accurate degree of dispersion of nanotubes in polymer matrices, a considerable number of classical and innovative analysis methods have emphasized the difficulty in obtaining an ideal dispersion.[11] However, for a large majority of these reports, the following scheme applies: examination of an intended property as function of the CNT concentration; furthermore, a critical concentration of CNTs, namely the percolation concentration, can be observed when the CNTs are responsible for a significant increase in the properties of the final composite.[4,7] It has been demonstrated that the decrease in the percolation concentration, which means increasing the

degree of dispersion, is strongly affected by the polarity of the partner material and the efficiency of their mixing methods.[3,4,7] From Ref. 9, the primary methods for obtaining a nanotube dispersion in polymers was recently reported by Grady[3]; this work attempts to illustrate how the first method, "Dispersion–Reaction," can be applied to achieve a better dispersion of CNTs. Several methods were investigated for dispersing the monomers, including CNTs in liquids with a low viscosity, water with surface-active agents, and followed by radical polymerization. A promising strategy would be to use the advantages of CNT noncovalent stabilization in the presence of surfactants[8,13] together with the "grafting-to" covalent functionalization that appeared due to the presence of radical initiators.[4,13] There are a considerable number of published reports in the area of monomer polymerization in an aqueous dispersion medium.[21–38] The initial monomer dispersions were performed in emulsions,[21–28] microemulsions,[29] dispersions,[30] suspensions,[34–38] and aqueous solutions.[39,40] The literature presents only a few works[21,31,32] for miniemulsion polymerization [styrene (St) and styrene-isoprene] in presence of single walled CNTs and none of them with MWCNTs for polystyrene (PS), St-acrylonitrile copolymer and polymethylmethacrylate matrixes. MWCNTs are less expensive and the aggregation tendency is still elevated for ultra long structures, therefore, the dispersion is quite restrictive. Using MWCNTs especially for the mentioned industrial polymers could bring several technological benefits in terms of applications in the materials side. Moreover, MWCNTs are more prone to be grafted in a one batch free radical polymerization because of their known wall defects; therefore, the interaction between filler and polymer matrix could be obtained in more profitable way.

Therefore in this study, from the best of our knowledge, we present for the first time the free radical polymerization of the mentioned monomers by miniemulsion in presence of MWCNT. After some preliminary experimental attempts (using suspension or emulsion method), the most adequate method for the radical polymerization of St, St-acrylonitrile, and methylmethacrylate (MMA) in presence of multiwalled carbon nanotubes (MWCNT) was determined to be miniemulsion polymerization. Under these conditions, the resulting latexes appear homogeneous without any considerable aggregation of the CNTs. The obtained composites were analyzed in terms of the degree of grafting of the polymers on the CNTs, thermal properties, and molecular weight of the nongrafted polymers. Finally, the resulting nanocomposites were foamed by the supercritical CO_2 technology and the effect of the CNTs on the quality of the foams morphology has been determined. The potentiality of these nanocomposite foams as electromagnetic interference (EMI) shielding materials has already been demonstrated.[41,42]

EXPERIMENTAL

Materials

The monomers (Sigma Aldrich), including St, MMA, and acrylonitrile, were purified by low pressure distillation at air pressure. The freshly distilled monomers were stored in a freezer until polymerization. Benzoyl peroxide (Bz_2O_2; Fluka), cetyltrimethylammonium bromide (CTAB; Sigma Aldrich), and hexadecane (Sigma Aldrich) were used as received without further purification. The carbon nanotubes (MWCNT-purified) produced by FutureCarbon GmbH were used as received.

Latexes Synthesis

A typical procedure for the polymerization was as follows: Mixture A, which contained different amounts of MWCNTs, was added to a surfactant-water mixture (between 0 and 2 wt % MWCNT [related to monomer content], 3.64 g of CTAB and 480.36 g of distilled water). The entire mixture was mechanically stirred for 10 min at 500 rpm (room temperature), and then an ultrasound treatment was applied (35,000 J for 10 min). A second mixture B, which contained 120 g of monomer, 8.86 g of initiator (Bz_2O_2), and 5 g of hexadecane, was prepared and kept in an ice bath after homogenization. Mixtures A and B were mixed and stirred for 30 min at 800 rpm, and then the system was placed in an ice bath and an additional ultrasound treatment was applied (265,000 J for 50 min). The entire polymerization mixture was transferred into an autoclave (equipped with a heating jacket, mechanical stirrer, steam condenser, and thermostat) and bubbled with nitrogen for 15 min. All polymerizations were performed under a nitrogen atmosphere at 400 rpm for several hours (starting with the regime temperature): for St, 90°C and 8 h; for methyl methacrylate, 90°C for 5 h; and for St-acrylonitrile (3 : 1 wt monomers ratio), 75°C for 3 h, then an increase from 75 to 82°C in 30 min and then 82°C in 2.5 h.

Foams Preparation

Depending on the polymer matrix, the foams have been prepared according to depressurization foaming (one-step) or solid-state foaming (two-step) processes. For both processes, polymer slices ($30 \times 12 \times 3$ mm^3) were introduced in a stainless steel high pressure autoclave (Parr instruments, 250 mL). For the one-step method, samples are saturated with CO_2 (999,998%, Air Liquide, Belgium) at 280 bar and at 105°C for 16 h in the case of styrene-acrylonitrile (SAN) copolymer samples. Foaming occurs during the fast depressurization step (4s). For the two-step process, the samples are saturated at 280 bar and at 40°C during 16 h to reach the CO_2 equilibrium before being quickly depressurized (4s). Then foaming occurred by placing the sample in a hot press during 3 min at 110°C in the case of PS samples or 120°C for poly(methyl methacrylate) (PMMA) samples.

Analyses

The distributions of the particle dimensions and average diameters were measured using a Malvern-Zetasizer Nano ZS instrument. After polymerization, a part of the latexes were kept to measure the particle dimensions by dynamic light scattering (DLS) and to obtain the electron microscopy images able to provide information about the interactions between the polymer matrix and the nanofillers. Environmental scanning electron microscopy images were obtained using a FEI-Quanta 200 instrument. Thermal analyses were performed using Q5000 for the thermogravimetric analysis (TGA) and a Q2000 for differential scanning calorimetry (DSC) both equipments from TA Instruments in a He atmosphere at a heating rate of 10°C

Figure 1. Homogeneity of the polymer-MWCNT nanocomposite latex achieved after using miniemulsion polymerization (latex based on SAN synthesized in the presence of 2% CNTs). [Color figure can be viewed in the online issue, which is available at wileyonlinelibrary.com.]

min^{-1}. Size exclusion chromatography was carried out in THF at 45°C at a flow rate of 1 mL min^{-1} with a SFD S5200 auto sampler liquid chromatograph equipped with a SFD refractometer index detector 2000. The PL-gel 5 μm (105, 104, 103, and 100 Å) columns were calibrated with PS standards for molecular parameter evaluation of PS and SAN samples and with PMMA standards for PMMA samples. Fourier transform infrared spectroscopy (FTIR) spectra were recorded from KBr pellets using a Bruker-Tensor 37 instrument. Separation of the grafted products was achieved by filtering the solid composite mixtures dispersed in THF for PS and SAN or in acetone for PMMA through 0.25 μm Millex-type membranes (Millipore). The foam porosity is determined by scanning electron microscopy (SEM) with a JEOL JSM 840-A instrument after metallization with Pt (30 nm). The average pore size was determined using the ImageJ v.1.45 software. The cell density[42] was calculated using the formula: $N_0 = (nM^2 \times A^{-1})^{3/2} \times \rho_S \times \rho_f^{-1}$. Where N_0 is the cell density, defined as the number of cells per unit volume of the original (unfoamed) polymer, n is the number of cells in the micrograph, A is the area of the micrograph, M is the magnification factor, ρ_S is the density of the solid samples, and ρ_f is the density of the foamed sample. Foam density (ρ_f) was calculated based on the measurement of the volumic expansion of the sample and its initial density ρ_S.

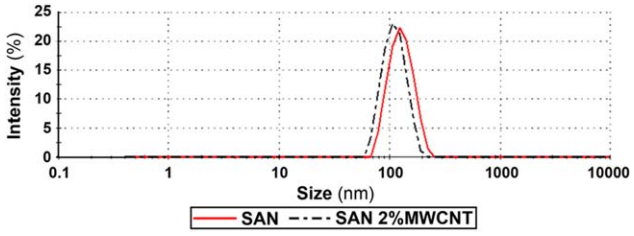

Figure 2. Decreasing of average particle sizes in presence of MWCNTs in comparison with blank polymer particles (miniemulsion polymerization for SAN or SAN in presence of 2% CNTs) in DLS profiles. [Color figure can be viewed in the online issue, which is available at wileyonlinelibrary.com.]

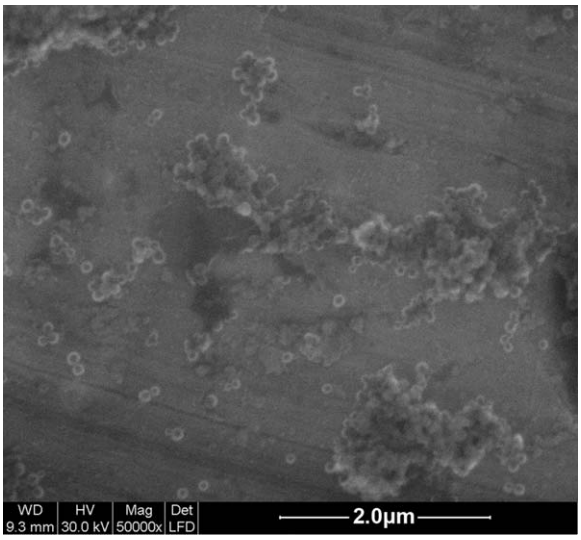

Figure 3. ESEM imaging of SAN particles (in the presence of 2% CNTs) supporting (indirectly) the details on shape and size range observed initially by DLS.

RESULTS AND DISCUSSION

To establish the formulations for the dispersed systems in this study, polymerization tests were performed also in emulsions

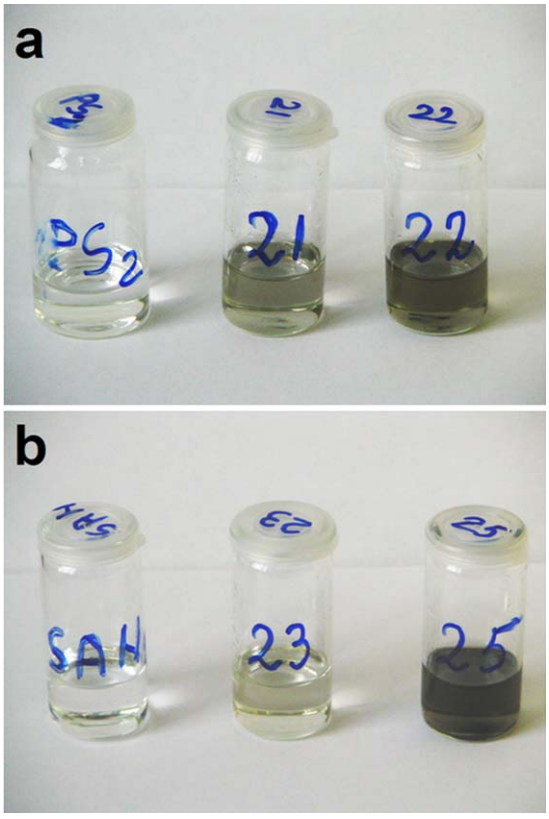

Figure 4. Hybrid dispersion aspect in N-methylpyrrolidone depending on the initial concentration of CNTs: (a) PS without CNTs, PS with 0.2% CNTs (21), respectively, with 1% CNT (22); (b) SAN without CNTs, SAN with 0.2% CNT (23), and with 1% CNTs (25). [Color figure can be viewed in the online issue, which is available at wileyonlinelibrary.com.]

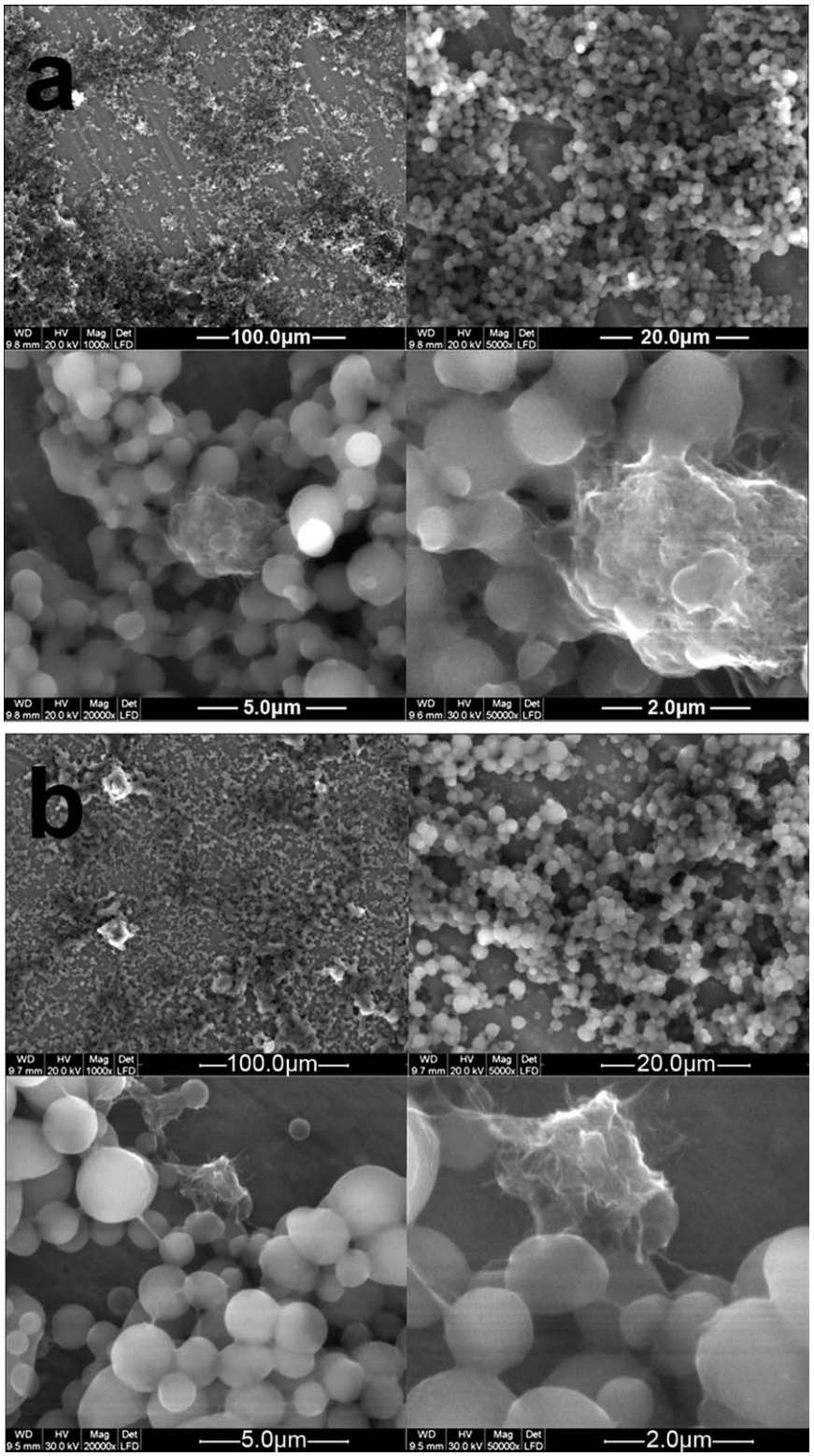

Figure 5. SEM images of hybrids with 2% CNTs dispersed in N-methylpyrrolidone dried by solvent evaporation (a: PS, b: SAN).

(sodium dodecylbenzenesulfonate as surfactant), suspensions ($CaCl_2$, Na_3PO_4 as stabilizer), and miniemulsions (CTAB, sodium dodecylbenzenesulfonate as surfactant).

The emulsion and suspension approaches ended with very unstable system and strong phase separation. The latex form in emulsion polymerization showed amounts of precipitated phase

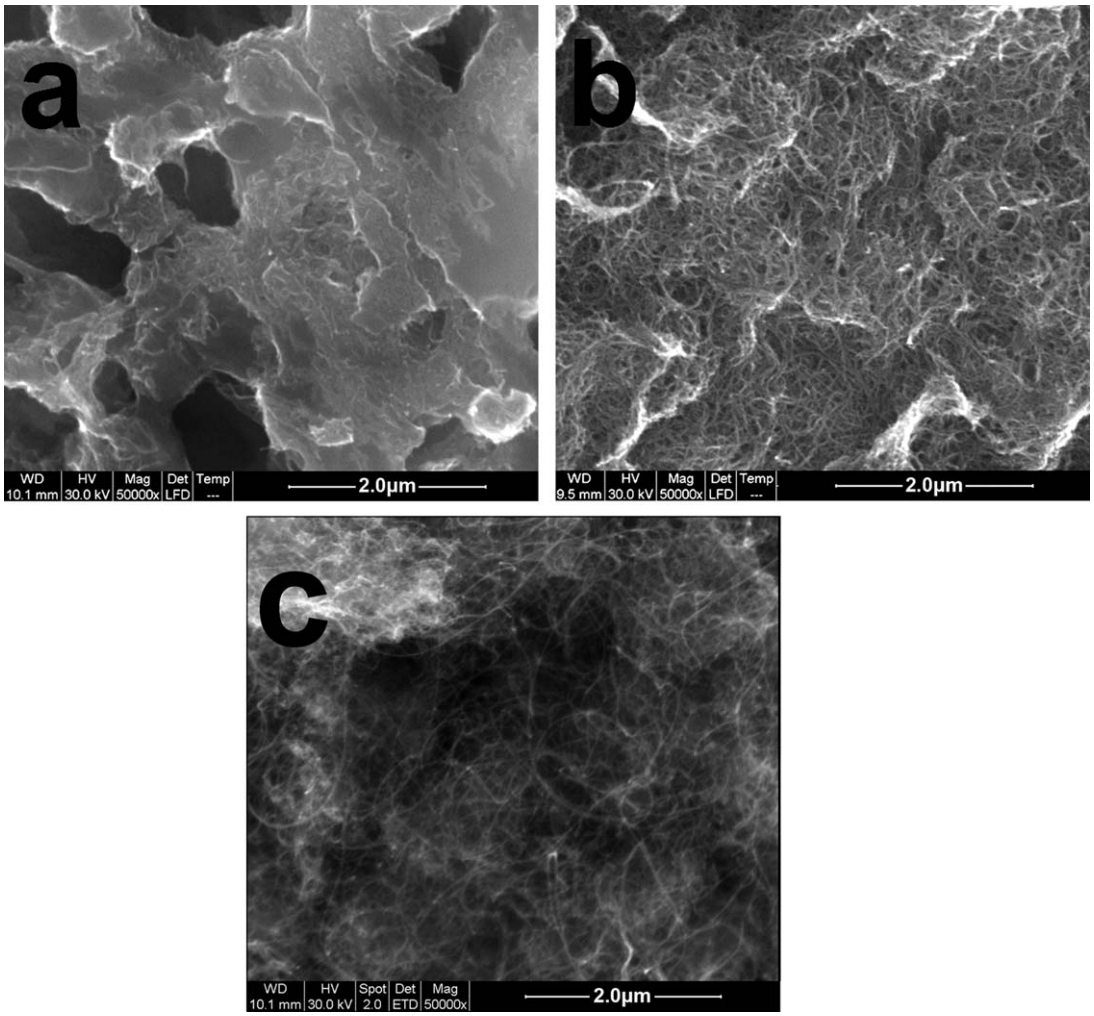

Figure 6. SEM images of PS and SAN copolymers grafted onto CNTs (CNT = 2 wt % vs. initial monomer content, a: PS, b: SAN) and (c) neat MWCNT.

and large amounts of coagulum. Suspension approach was also inappropriate and during the polymerization the stirrer remained trapped in the polymer precipitated phase. Contrary miniemulsion technique especially with CTAB as surfactant, allowed the obtaining of homogenous (crude) miniemulsions and latexes (Figure 1). The stability was high enough to allow DLS measurements (Figure 2). To asses (only) the polymer particles dimensions dilution was necessary (context of high solid content and possible interference of the large MWCNT particles). The obtained latexes by miniemulsion polymerization did not showed phase separation even when were subject to dilution in DLS measurements.

The preliminary results are in good agreement with previously published data.[21,22] In the mentioned miniemulsions, anionic surfactants migrate from the CNTs to monomer-polymer particles, which induce agglomeration of the nanofiller.[21,32] For the latexes-CNT mixtures dispersed in water using surface-active

Table I. The Influence of CNT Concentration on Latex Particles Dimension (Dmed), Molecular Parameter of the Produced Polymers (Mn, PDI) and Grafted Copolymer Concentration

	PS				SAN				PMMA			
MWCNT (%wt)	0	0.2	1	2	0	0.2	1	2	0	0.2	1	2
Dmed (nm)	220	131	-	115	122	-	108	106	122	91	68	91
Mn $\times 10^3$ (g/mol)	23.4	26.4	36.7	43.9	59.1	48.2	83.4	56.2	-	85.9	98.9	127.7
PDI (M_w/M_n)	1.97	2.07	2.15	2.5	3.04	2.79	2.89	2.42	-	4.4	3.8	7.7
Grafted CNT (gCNT/gPolymer)	-	-	0.39	2.43	-	0.07	1.14	4.25	-	0.57	2.45	4.9

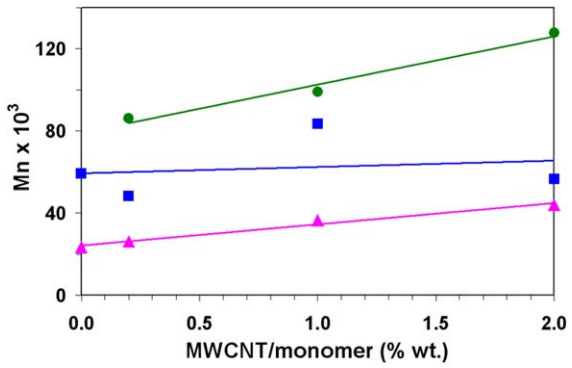

Figure 7. Evolution of the number average molar masses of the nongrafted polymers with the initial concentration of MWCNTs. [Color figure can be viewed in the online issue, which is available at wileyonlinelibrary.com.]

agents, the highest concentration of CNT homogeneously dispersed over the polymer surfaces was obtained with cationic surfactants (in good agreement with the literature).[43]

Studies regarding heterogeneous systems stabilized on CNTs are sustaining that both o/w systems[23] and w/o systems[44] can be stabilized through a Pickering mechanism. In the initial monomer polymerization systems, the CNTs can be dispersed in both oil and the aqueous phase.[23] Even if a portion of the CNTs remain apparently in the aqueous phase after the polymerization process, through a good affinity with polymer surfaces,[44] these do not agglomerate themselves and ensures homogeneity of the final mixture.[38]

The analysis of the dimensions of particles obtained in the miniemulsions confirms that submicrometric dimensions can be obtained as well for polymer latex particles in presence of MWCNT. This phenomenon was verified in literature only for SWNT and some polymer latexes.[5,21,31] The results were obtained both in liquid media by DLS (Figure 2) and in dry phase as well by SEM (Figure 3) investigations. The particles dimensions (DLS) are referring only to the latex particles and not to the MWCNTs or MWCNTs polymer aggregates. The same was done for the morphological imaging by SEM. Even

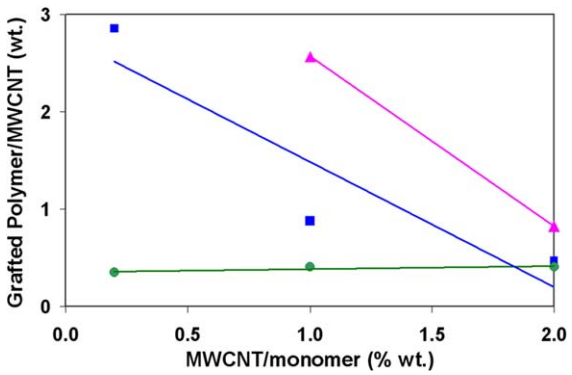

Figure 8. Evolution of the percentage of grafted (co)polymer toward initial monomers with the initial concentration of the MWCNTs. [Color figure can be viewed in the online issue, which is available at wileyonlinelibrary.com.]

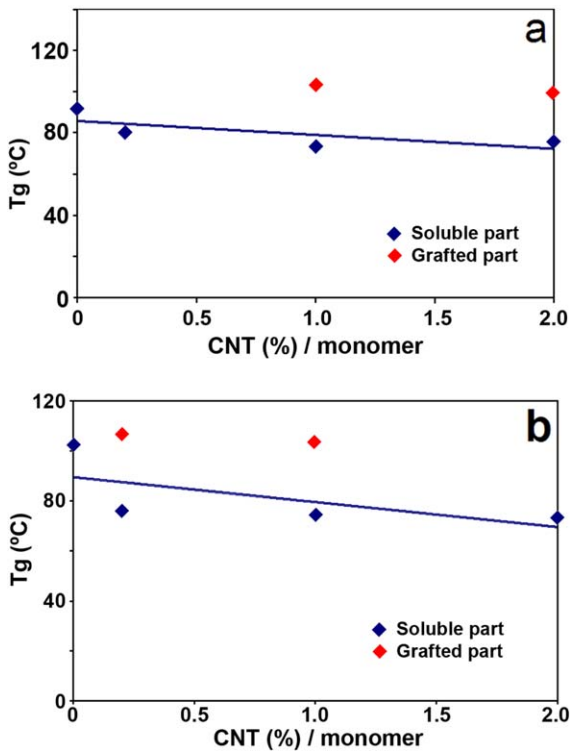

Figure 9. Influence of CNT concentration initially added to the polymerization medium on the glass transition temperature value (T_g) of the soluble (nongrafted) and grafted polymers (a: PS, b: SAN). [Color figure can be viewed in the online issue, which is available at wileyonlinelibrary.com.]

after dilution, the aggregation in solid state was quite strong (Figure 3). Only some individual particles could be seen and confirmed indirectly the DLS results. The slight decrease in particle sizes suggest even at this point a possible decrease in the monomer feed for the spherical latex particles (Figure 2). In the next analyses, this aspect was confirmed to be happened since grafted polymer phase occurred on the MWCNTs.

The major component of the latexes was separated from the aqueous phase by filtration, and after drying, it was used to analyze the degree of grafting, measure the molecular masses of the nongrafted polymer and to investigate its ability to form foams when soaked in supercritical CO_2.

During the radical polymerization of vinyl monomers in dispersed systems, the interactions between CNTs and the obtained polymer particles can be noncovalent[8,15,43] or covalent with the formation of grafted copolymers.[26–28,34,35,37,38,40]

The formation of grafted copolymers occurs because of the addition of radicals, which are produced through the thermal decomposition of initiators, to CNT double bonds. The degree of grafting is affected by the reactivities of the radical and initiator[26,35,45,46] and also by the solvation capacity of CNT by monomers.[40]

Another evidence discussed in the literature, regarding the formation of grafted copolymers on the CNTs would be the stability of the CNTs from hybrids in the polymer solvents.[25,29,47] In

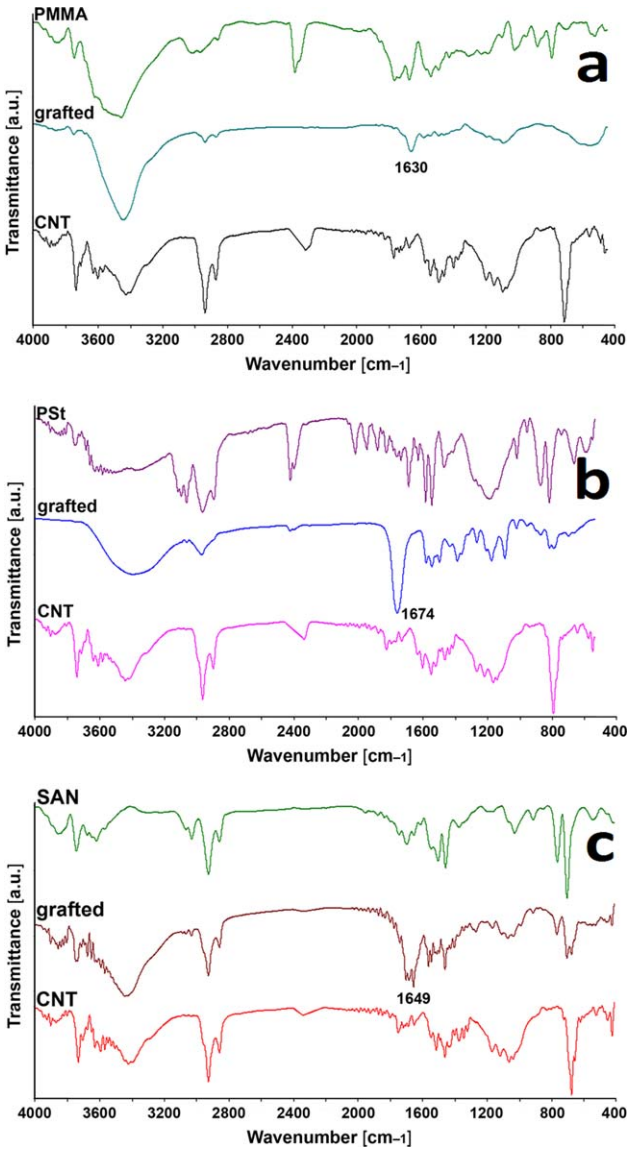

Figure 10. FTIR spectra of PMMA (a), PS (b), SAN (c), and the CNT grafted with these (co)polymers. [Color figure can be viewed in the online issue, which is available at wileyonlinelibrary.com.]

the conditions used in this study, a similar phenomenon could be observed (Figure 4) in which hybrid dispersions of PS (a) and SAN (b) in N-methylpyrrolidone provide a good stabilization for the CNTs and their color accentuates with the increasing concentration of CNTs. The dispersions are completely stable (stability was verified for more than 10 months). After dilution and drying, these hybrids present micron sized polymer particles as well as some agglomerations from which we can observe the CNTs (Figure 5). These hybrids are showing also the ability of the grafted MWCNTs to connect the free polymer phase. As it can be observed (Figure 5), the spherical particles are connected either by contacts or by thin wire like phases. These results are in good agreement with the PS-SWCNTs reported in literature obtained also by miniemulsion polymerization.[32]

To separate the grafted copolymers from the non-grafted polymers, the latexes were dissolved in THF and the hybrid dispersion was isolated by filtration through 0.25 μm membranes. After these separations, grafted copolymers that contain a high concentration of CNTs are completely different from the images presented in Figure 5. Figure 6 illustrates that the CNTs do not have an excess of nongrafted polymers and that the nanofillers are surrounded by one polymer layer. Another aspect revealed by SEM (Figure 6) analysis on grafted nanotubes was the marginal effect on nanofiller length in the sonication step.

Using the aforementioned filtration techniques, the nongrafted polymers could be separated from the grafted ones (Table I). Efficient analyses were performed for the two fractions to highlight the influence of the nanofiller. From the analysis of the data in Table I and Figure 7, it can be stated that increasing the concentration of CNTs would affect the molar masses of the non-grafted polymers, the polydispersity index (M_w/M_n), and the composition of the obtained grafted copolymers. This was observed in the literature on SWCNTs, graphite, bulk or suspension polymerization.[21,35,38,45,46]

As shown in Figure 7, when increasing the concentration of the CNTs, the M_n value of the nongrafted polymers will increase in the order of PMMA > SAN > PS. Simultaneously, the amount of grafted polymers related to the initial monomers decreases with increasing concentration of CNTs in the order of PS > SAN > PMMA (Figure 8). Thermogravimetric analyses allowed the amount of the obtained grafted copolymers to be determined (Table I, Figure 8).[25–29,35,36,39,45–47]

The explanation of results in Figures 7 and 8 is based on two processes. First during the consumption of radicals produced by the decomposition of the initiators, a part of the radicals are absorbed by addition to the double bonds of the CNTs.[21,38,40,45,46] Therefore, the radicals available for initiation of the monomer in droplets are decreasing as the concentration of the CNTs increases. Second, for the MWCNTs from the polymerization medium, the dispersible monomer layer used for solvation is limited by the structure of the monomer.[40] St has a high solvation capacity of CNTs due to π electrons from aromatic nucleus, which provides a considerable opportunity to form grafted copolymers and simultaneously initiate with the radicals produced by the homolytic scission of the initiator. In the case of MMA, its interaction with the CNTs is lower, and the majority of the initiator radicals are consumed by addition to the CNTs, which determines a minimum grafting degree and maximum molecular mass in comparison with the rest of the studied monomers.

Using DSC analyses, it was possible to follow the modification of the glass transition temperature value of the polymers soluble in solvent (nongrafted) and grafted ones. These modifications are presented in Figure 9. The T_g values were calculated only PS and SAN since for PMMA grafted phase, the very low amounts did not allowed measurements.

The influence of the concentration of MWCNTs is minor, as evidenced by the data presented in Figure 9. A slight decrease of the T_g value for the nongrafted polymers along with the increasing nanofiller concentration can be an effect of the formation of oligomers with plasticizer character.[35]

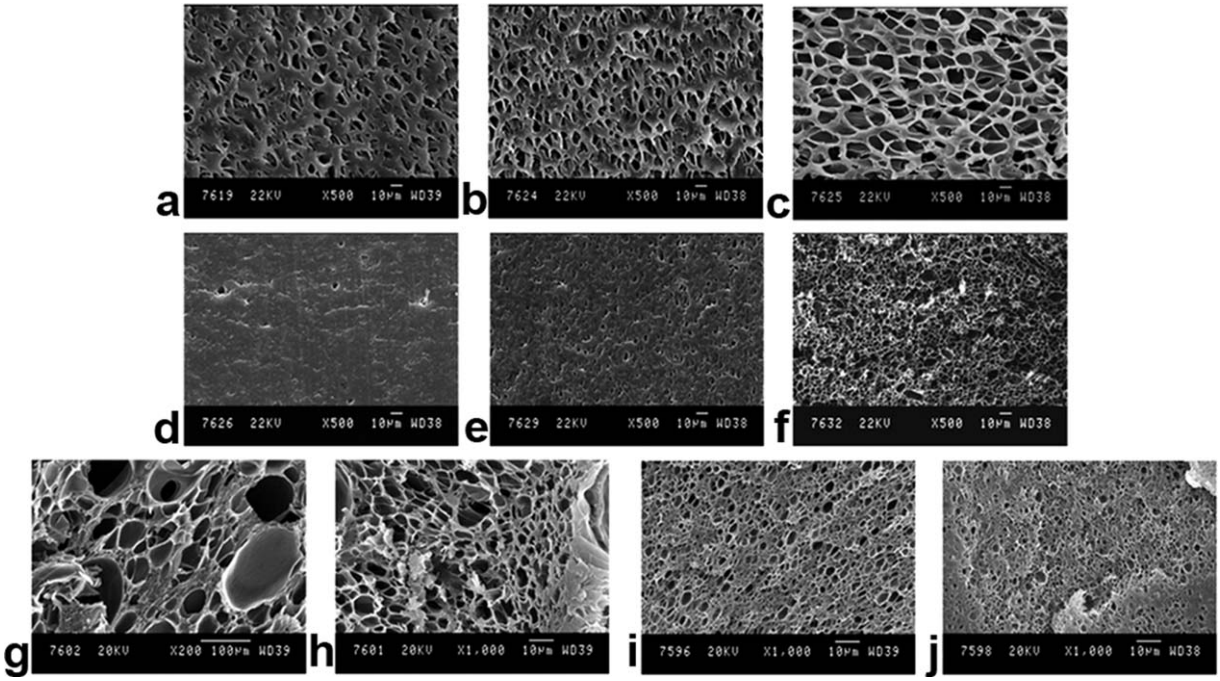

Figure 11. SEM micrographs of (a) SAN, (b) SAN + 0.5 wt % CNTs, (c) SAN + 1 wt % CNTs, (d) PS, (e) PS + 0.5 wt % CNTs, (f) PS + 1 wt % CNTs, (g) PMMA, (h) PMMA + 0.2 wt % CNTs, (i) PMMA + 1 wt % CNTs, and (j) PMMA + 2 wt % CNTs.

The most interesting observations resulted from the data presented in Figure 9, refers to polymers grafted on the CNTs. If the amount of CNT's used in the synthesis increases with respect to monomer level the T_g's are decreasing. This happens either by the change in nature of the grafted phase (grafted molecules density or partial crosslinking) or by the increasing of the radicals transfer on the CNT's walls. These results are consistent with previously published data with similar systems (with carbon black, by bulk-suspension process, aqueous deposition polymerization method, or with SWCNTs).[23,25,36,39,48]

FTIR spectroscopy is an appropriate method for determining the formation of grafted polymer on CNTs surface.[37,46,49] The formation of the final PMMA/CNT grafted phase is confirmed by a specific absorptions [Figure 10(a)] shown as the appearance of a new peak at 1630 cm^{-1}. This band was not present in the spectrum of PMMA or CNT's. This absorption occurrence is precisely described in literature to belong to the C—C of grafted PMMA chains on CNTs.[50] The rest of the peak positions belonging to PMMA were found shifted in grafted PMMA indicating a completely different confinement of the chains in comparison with pure polymer. In PS grafted on CNT structures, the specific absorption band was again found with high intensity at 1674 cm^{-1} [Figure 10(b)]. This indicates according to the existing literature the covalent attaching of the polymer chains to CNT's walls.[37,49,51,52] Grafted polymer chains exhibits different absorptions for the C—C stretching vibrations in comparison with initial PS.[44] Also, the rest of the bands absorptions were found by different small shifts in the peak positions.[53] In the case of SAN/CNT's [Figure 10(c)] the same specific absorption at 1647 cm^{-1} was found sustaining the same covalent attaching of the chain molecules.

The possibility to prepare microcellular polymer/CNTs foams starting from the different nanocomposites prepared by miniemulsion has been envisioned. Indeed, these kinds of foams have received great interest due to their potential use in various applications such as electrostatic dissipation and EMI shielding. To be efficient, the foams must exhibit low density and low pore size. Two different foaming procedures have been envisioned, that is, the depressurization process and the solid-state process. In the first method, the CO_2 impregnation is performed at a temperature

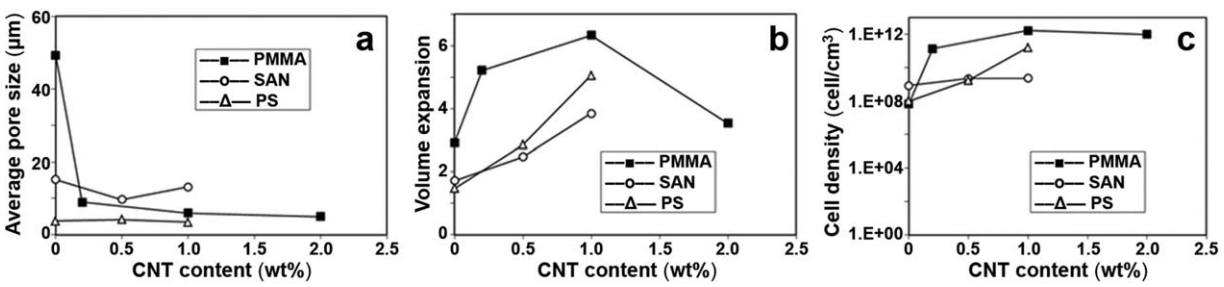

Figure 12. (a) average pore size, (b) volume expansion, and (c) cell density as a function of frequency of PS, PMMA, and SAN foams.

close or above the glass transition (or melting in case of semicrystalline polymer) temperature. The cell nucleation and the cell growth then occur during the depressurization step. In the second technique, the polymer sample is saturated with CO_2 at low temperature preventing any cell growth during the pressure release. The foaming then occurs during an elevation of the temperature. Figure 11 shows the SEM micrographs of PS, SAN and PMMA foamed in their respective optimal conditions, that is, the depressurization process for SAN (foaming temperature = 105°C) and the solid-state foaming for PS (foaming temperature = 110°C) and PMMA (foaming temperature = 120°C). The presence of CNTs clearly improves the foam morphology with more uniform cells. The influence of MWCNT on the morphology of foams is different, also due to the different polymer matrixes. In PS and SAN matrixes, the compatibility induced by the grafting phase allows apparently more uniform pores meanwhile in PMMA matrix the tendency was reduced. Judging also by the polarity differences of the polymer matrixes, the nucleating effect is stronger on the morphology of as the polarity difference between filler and matrix increases. The nucleation effect of CNTs is noticeably observed with a significant decrease in average cell size [Figure 12(a)] and an important improvement of the cell density [Figure 12(b)] when the CNTs content is increased. Moreover, the presence of CNTs limits the coalescence and/or collapse of the cells, particularly in the case of PMMA, which allows improving the volume expansion of the foams [Figure 12(b)]. When the CNTs is further increased beyond 1 wt %, the volume expansion decreased probably due to the increase of viscosity induced by the presence of CNTs, which limit the cell growth during the foaming. The foams obtained with the three different matrices at 1 wt % content of CNTs possess all a low density (< 0.3 g/cm^3), low pore size (< 10 μm) and high cell density ($> 10^9$ cell/cm^3).

CONCLUSIONS

Miniemulsion polymerization was proven as useful tool for achieving homogenous polymer-MWCNT nanocomposites in latex form as well as in solid state. The final polymer was found in particles state (latex particles) as well as grafted on the MWCNTs. The benefits in terms of MWCNT dispersion was indirectly proven by the associated materials ability to provide uniform pores distribution during foaming process. The isolated polymer grafted MWCNT showed stable and homogenous dispersions (with solution appearance) in the polymer solvent. The molar masses of the polymers are increasing proportional with degree of grafting. As a consequence of the process the T_g's of the free polymers are decreasing and the T_g's of the grafted polymers are almost constant with MWCNT concentration. Grafted polymers showed specific bands in FTIR indicating the specific interaction between polymer chain and MWCNT's body. The foam materials obtained with the mentioned nanocomposites showed a decrease of pore sizes, an increase in cell density and higher volume expansion when the MWCNTs concentration increases.

ACKNOWLEDGMENTS

This work was financially supported by the project "High Aspect Ratio Carbon-based Nanocomposites" (HARCANA) within the European Community's 7th Framework Programme for Research and Technological Development under the Grant Agreement number NMP3-LA-2008-213277. J.-M.T., M.A., and C.J. thanks the Belgian Science Policy Office (BELSPO) for financial support through the Interuniversity Attraction Pole program (PAI VII/05). J.-M.T. thanks FNRS for financial support.

AUTHOR CONTRIBUTIONS

Dr Donescu supervised the research and wrote the manuscript main line; Dr Corobea established the experimental set-up, performed the synthesis experiments, reviewed and edited the manuscript, submitted the manuscript; Dr Petcu perfomed the grafted phase separations; Dr Spataru performed the TGA experiments; Dr Ghiurea performed the SEM (all the investigations excluding the foam section); Dr Somoghi performed the FTIR measurements and interpretations, Gabor perfomed the DSC measurements; Dr Thomassin performed the size exclusion chromatography; Prof Alexandre performed the foam obtaining and helped in the foam section writting; Dr Jerome performed the foams characterization and SEM studies.

REFERENCES

1. Iijima, S. *Nature* **1991**, *354*, 56.
2. Mittal, V. Polymer Nanotube Nanocomposites: Synthesis, Properties, and Applications; Wiley-Scrivener: Salem, **2010**.
3. Grady, B. P. *Macromol. Rapid Commun.* **2010**, *31*, 247.
4. Ma, P. C.; Siddiqui, N. A.; Marom, G.; Kim, J. K. *Compos. A* **2010**, *41*, 1345.
5. Landfester, K.; Weiss, C. K. *Adv. Polym. Sci.* **2010**, *229*, 1.
6. Wang, T.; Keddie, J. L. *Adv. Colloid Interface Sci.* **2009**, *147*, 319.
7. Bauhofer, W.; Kovacs, J. Z. *Compos. Sci. Technol.* **2009**, *69*, 1486.
8. Hu, C. Y.; Xu, Y. J.; Duo, S. W.; Zhang, R. F.; Li, M. S. *J. Chin. Chem. Soc.* **2009**, *56*, 234.
9. Rana, S.; Alagirusamy, R.; Joshi, M. *J. Reinf. Plast. Compos.* **2009**, *28*, 461.
10. Winey, K. I.; Vaia, R. A. *MRS Bull.* **2007**, *32*, 314.
11. Schaefer, D. W.; Justice, R. S. *Macromolecules* **2007**, *40*, 8501.
12. Bokobza, L. *Polymer* **2007**, *48*, 4907.
13. Tasis, D.; Tagmatarchis, N.; Bianco, A.; Prato, M. *Chem. Rev.* **2006**, *106*, 1105.
14. Coleman, J.; Khan, U.; Blau, W.; Gunko, Y. *Carbon* **2006**, *44*, 1624.
15. Grossiord, N.; Loos, J.; Regev, O.; Koning, C. E. *Chem. Mater.* **2006**, *18*, 1089.
16. Shaffer, M. S. P.; Sandler, J. K. W. In Processing and Properties of Nanocomposites; Advani, S. G., Eds.; World Scientific Publishing Co. Pte. Ltd: Singapore, **2007**; Chapter *1*, p 1–60.
17. Esawi, A. M. K.; Farag, M. M. In Polymer Nanotube Nanocomposites: Synthesis, Properties and Applications; Mittal, V., Eds.; Wiley-Scrivener: Salem: **2010**; Chapter *15*, p 423.

18. Ianchis, R.; Corobea, M. C.; Donescu, D.; Rosca, I. D.; Cinteza, L. O.; Nistor, L. C.; Vasile, E.; Marin, A.; Preda, S. *J. Nanopart. Res.* **2012**, *14*, 1.
19. Ianchis, R.; Donescu, D.; Corobea, M. C.; Petcu, C.; Ghiurea, M.; Serban, S.; Radovici, C. *Colloid Polym. Sci.* **2010**, *288*, 1215.
20. Ianchis, R.; Cinteza, L. O.; Donescu, D.; Petcu, C.; Corobea, M. C.; Somoghi, R.; Ghiurea, M.; Spataru, C. *Appl. Clay Sci.* **2011**, *52*, 96.
21. Ha, M. L. P.; Grady, B. P.; Lolli, G.; Resasco, D. E.; Ford, W. T. *Macromol. Chem. Phys.* **2007**, *208*, 446.
22. Xia, H.; Qiu, G.; Wang, Q. *J. Appl. Polym. Sci.* **2006**, *100*, 3123.
23. Menner, A.; Verdejo, R.; Shaffer, M.; Bismarck, A. *Langmuir* **2007**, *23*, 2398.
24. Kim, T. H.; Doe, C.; Kline, S. R.; Choi, S. M. *Adv. Mater.* **2007**, *19*, 929.
25. Casado, R. M.; Lovell, P. A.; Navabpour, P.; Stanford, J. L. *Polymer* **2007**, *48*, 2554.
26. Shaffer, M. S. P.; Koziol, K. *Chem. Commun.* **2002**, *18*, 2074.
27. Wu, H. X.; Qiu, X. Q.; Cao, W. M.; Lin, Y. H.; Cai, R. F.; Qian, S. X. *Carbon* **2007**, *45*, 2866.
28. Cheng, Z.; Pan, Q.; Rempel, G. L. *J. Polym. Sci. Part A: Polym. Chem.* **2010**, *48*, 2057.
29. Patole, A. S.; Patole, S. P.; Yoo, J. B.; Ahn, J. H.; Kim, T. H. *J. Polym. Sci. Part B: Polym. Phys.* **2009**, *47*, 1523.
30. Kara, S.; Arda, E.; Dolastir, F.; Pekcan, O. *J. Colloid Interface Sci.* **2010**, *344*, 395.
31. Lu, H. F.; Fei, B.; Xin, J. H.; Wang, R. H.; Li, L.; Guan, W. C. *Carbon* **2007**, *41*, 936.
32. Ham, H. T.; Choi, Y. S.; Chee, M. G.; Chung, I. J. *J. Polym. Sci. Part A: Polym. Chem.* **2006**, *44*, 573.
33. Reyes, Y.; Paulis, M.; Leiza, J. R. *J. Colloid Interface Sci.* **2010**, *352*, 359.
34. Park, S. J.; Cho, M. S.; Lim, S. T.; Choi, H. J.; Jhon, M. S. *Macromol. Rapid Commun.* **2005**, *26*, 1563.
35. Lopes, C. N.; Moreira, R. F. P. M.; Machado, R. A. F.; Araujo, P. H. H. *Macromol. Symp.* **2005**, *229*, 72.
36. Zaragoza-Contreras, E. A.; Lozano-Rodriguez, E. D.; Roman-Aguirre, M.; Antunez-Flores, W.; Hernandez-Escobar, C. A.; Flores-Gallardo, S. G.; Aguilar-Elguezabal, A. *Micron* **2009**, *40*, 621.
37. Kwon, S. M.; Kim, H. S.; Kim, D. Y.; Yun, Y. S.; Jin, H. J. *J. Appl. Polym. Sci.* **2008**, *110*, 3737.
38. Slobodian, P. In Polymer Nanotube Nanocomposites: Synthesis, Properties and Applications; Mittal V. Eds.; Wiley-Scrivener: Salem, **2010**; Chapter *8*, p 221.
39. Zhang, H.; Xu, L.; Yang, F.; Geng, L. *Carbon* **2010**, *48*, 688.
40. Ford, W. T. *Macromol. Symp.* **2010**, *297*, 18.
41. Thomassin, J. M.; Pagnoulle, C.; Bednarz, L.; Huynen, I.; Jerome, C.; Detrembleur, C. *J. Mater. Chem.* **2008**, *18*, 792.
42. Thomassin, J. M.; Vuluga, D.; Alexandre, M.; Jerome, C.; Molenberg, I.; Huynen, I.; Detrembleur, C. *Polymer* **2012**, *53*, 169.
43. Jin, H. J.; Choi, H. J.; Yoon, S. H.; Myung, S. J.; Shim, S. E. *Chem. Mater.* **2005**, *17*, 4034.
44. Wang, H.; Hobbie, E. K. *Langmuir* **2003**, *19*, 3091.
45. Capek, I.; Kocsisova, T. *Polym. J.* **2011**, *43*, 700.
46. Park, S. J.; Cho, M. S.; Lim, S. T.; Choi, H. J.; Jhon, M. S. *Macromol. Rapid Commun.* **2003**, *24*, 1070.
47. Qin, S.; Qin, D.; Ford, W. T.; Herrera, J. E.; Resasco, D. E.; Bachilo, S. M.; Weisman, R. B. *Macromolecules* **2004**, *37*, 3965.
48. Grady, B. P.; Paul, A.; Peters, J.; Ford, W. T. *Macromolecules* **2009**, *42*, 6152.
49. Shanmugharaj, A. M.; Bae, J. H.; Nayak, R. R.; Ryu, S. H. *J. Polym. Sci. Part A: Polym. Chem.* **2007**, *45*, 460.
50. Manhong, L.; Tao, Z.; Zichen, L.; Zhongfan L. *J. Phys. Chem. C* **2009**, *113*, 9670.
51. Peng, L. *J. Nanopart. Res.* **2009**, *11*, 1011.
52. Baibarac, M.; Baltog, I.; Lefront, S.; Mevellec, J. Y.; Bucur, C. *Diamond Relat. Mater.* **2008**, *17*, 1380.
53. Espinosa-Gonzalez, C. G.; Rodriguez-Macias, F. J.; Cano-Marquez, A. G.; Kaur, J.; Shofner, M. L.; Vega-Cantu, Y. I. *J. Mater. Res.* **2013**, *8*, 1087.